Performance Analysis of Instruments Used to Measure Stress Change Resulting from Mining

Mark K. Larson
Bo-Hyun Kim
CDC, NIOSH, Spokane

ABSTRACT

Researchers at the National Institute for Occupational Safety and Health (NIOSH) have advocated the use of instrumentation in underground mine ground control studies to aid in understanding failure mechanisms and to calibrate numerical models. The purpose of these efforts is to reduce accidents and fatalities in underground mines resulting from inadequate design of mining layout or supports. A recent examination of some results of stress change measurement raised some questions about the validity of elastic solutions in ground, such as coal. Particularly under deep cover as is prevalent in the western United States, the coal around a borehole would likely have yielded so that post-yield behavior would govern the response of the instrument.

A numerical experiment was conducted by NIOSH researchers using the FLAC software (Itasca Consulting Group, 2016) to investigate the response of the borehole pressure cell (BPC) and the biaxial stressmeter to varying degrees of plastic behavior. The pre-encapsulated BPC cell pressure exhibits increasing departure from the elastic case with decreasing post-peak-strength slope of the stress-strain curve. On the other hand, because the BSM usually provides much more confinement to the surrounding rock than does the BPC, the measurements obtained from the BSM do not depart significantly from the changes in secondary principal stresses and directions as calculated by the elastic solution.

INTRODUCTION

Several years ago, Larson et al. (2000) described several instruments that NIOSH had used in underground field studies and how to monitor them with dataloggers. This information is still relevant because of the need to understand how excavation affects the stability of mines and thus, the safety of mining personnel. One class of instruments described in that paper includes those instruments that measure change in rock stress. Although several such instruments might be used to measure stress change, the focus of this paper is on two instruments with which NIOSH has had more recent experience—the borehole pressure cell (BPC) (Geokon, 2018a; RST Instruments, 2018) and the biaxial stressmeter (BSM) (Geokon, 2018b). Other instruments, such as the CSIRO hollow inclusion stress cell (HICell) (Earth Sciences, 2019; Worotnicki and Walton, 1976) may be included in future studies.

Early studies in the development of the BPC were those of Panek and Stock (USBM, 1964), Sellers (1970), Lu (1984), and Babcock (1986). Babcock's work is particularly useful, but his setting and testing range was far below what we experienced in the NIOSH study, and it was Babcock's data reduction scheme from his laboratory experiments that was used to calculate stress change in the NIOSH study (NIOSH, 2019a).

Su and Hasenfus (1990) conducted a laboratory and numerical investigation of the BPC. They performed uniaxial tests on a nylon block with a BPC installed at two different setting pressures in a hole in the block. The responses had different degrees of nonlinearity, according to the setting pressure. These results prompted use of a nonlinear finite element model to simulate the response of a medium representing weak, soft coal. Although the mesh might be considered somewhat coarse compared to more modern practices, the results are significant for the current study. The ratio of applied stress change to cell pressure (K-factor) increased with increasing setting pressure and decreasing medium modulus. Moreover, the K-factor for the weak coal varied from 1.2 at 13.79 MPa (2,000 psi) to 1.485 at 57.92 MPa (8,400 psi), showing a range of applied stress in which there would be a significant increase of inelasticity in the coal.

Borehole pressure cells have been used in several studies to investigate changes in stress associated with mining (DeMarco, Koehler, and Lu, 1988; Estey, 1995; Koehler et al., 1996; Larson et al., 1995; Larson and Whyatt, 2012; Lu, 1986; Pariseau, 2007; Pariseau, McCarter, and McKenzie, 2008; Tadolini and Barczak, 2008; USBM, 1995; Vandergrift and Conover, 2010; Westman et al., 1995; Westman, Molka, and Conrad, 2016; Wright, Howell, and Dearinger, 1979). In most cases, the researcher or engineer assumed the cell pressure change of a BPC to be equivalent to the change in rock stress. Vandergrift and Conover (2010) and Larson

and Whyatt (2012) are among those who applied a data reduction scheme to field data, along with an assumption that the ratio of horizontal stress change to vertical stress change is constant. Vandergrift and Conover (2010) provide an excellent description of such an application, the Babcock data reduction scheme, with that assumption.

The biaxial stressmeter, model 4350BX from Geokon, is a hollow cylinder made of high-strength steel. Vibrating wire sensors measure diameter change, longitudinal strain, and temperature for the 10-gauge cell, which the authors of this paper much prefer over the four-gauge instrument that has no redundancy and no measurement of axial strain. The user inserts the instrument into a borehole that is filled partially with grout so that the instrument becomes fully encapsulated by grout when its orientation and depth are set. To that end, a sufficient working time of the grout is essential.

It is beyond the scope of this paper to provide details of the sensor technology. However, NIOSH has had good experiences in using both the BPC and the BSM with a datalogger monitoring the sensors. In the case of the BPC, various types of pressure transducers may be located in the mine opening outside of the borehole to monitor instrument response. Because the relatively soft hydraulic system most affects the overall instrument stiffness, it can be helpful to keep the length of hydraulic lines of all BPCs at a site constant.

PROBLEM STATEMENT

This paper is the result of questions arising from a field study whose detailed results were submitted for publication (NIOSH, 2019a, 2019b). In that investigation, BPCs were used to monitor stress change in pillars, a barrier pillar, and in the next panel as a longwall face approached and passed the instruments. For that study, the stress change calculated from cell pressure measurements according to either standard method resulted in stress change that was greater than what was possible, even if the weight of all of the panel overburden were transferred fully to the abutment. This result caused some question about how post-peak strength deformation around the borehole affected the response of the instrument. Moreover, if the BPCs were so affected, the question was equally important concerning another instrument with which NIOSH has had good experience—the BSM.

NUMERICAL EXPERIMENTS

Models were constructed to simulate both the BPC and the BSM. For the purposes of this study, the model was simplified to be two-dimensional with plane strain. Therefore, the finite-difference code, FLAC (Itasca Consulting Group, 2016), was used to simulate various conditions of the rock mass. FLAC has elasto-perfectly plastic (Mohr-Coulomb) and strain-softening constitutive models, which are sufficient for simulating various degrees of post-peak strength behavior.

Borehole Pressure Cell Simulation of Babcock's Radial Pressure Tests

The first step in our approach was to attempt to simulate the radial experiments of Babcock (1986) with a model built and run with FLAC. For brevity of space, we will not describe the model or the approach. However, the results were disappointing in that our method of loading the platens in the numerical model did not account for the seating and changing contact area between the flatjack and the grout platens in the experiment where only one BPC was used for all tests (Tadolini, 2019). However, at higher setting pressure, the laboratory and numerical model responses were much closer to each other. Although we were unable to simulate the laboratory results, and because our objective was not to determine calibration constants, we proceeded with more numerical experiments to determine the effect of various degrees of yielded host material on the instrument response.

Borehole Pressure Cell Simulation of Hypothetical Field Loading

A hypothetical field loading case was designed to be similar to the field situation where cell pressure was much higher than the level of stress change that was possible (NIOSH 2019a, 2019b). For this experiment, we used coal for a host material, having Young's modulus of 3.45 GPa (500,000 psi) and Poisson's ratio of 0.25. The value used for Young's modulus of the coal is greater than that of most coals, but not out of range of some western coals. Because the purpose of our study is not calibration, but to examine the effect of inelasticity of the host material on the instrument response, such a high value does not lessen the probability of reaching our objective. Mine Backer Grout was used for the platens with properties. Four samples were tested with strain gauges at 13 days, 19 days, and two and 20-days because of availability of personnel and equipment. Results had no correlation to age. Standard deviations of Young's modulus and Poissons ratio as a percentage of the mean were 3.11% and 0.66%, respectively. The model grid was modified to facilitate vertical and horizontal stress loading, as shown in Figure 1 and Figure 2.

For this model, the platen grid was assigned the null constitutive model until the hole came to equilibrium. This means that the model calculations proceeded as if nothing were in the borehole until initial equilibrium was established. To accomplish the initial stress state, the sides and the top and bottom were loaded with small constant-stress increments until stresses applied were –17.46 MPa (–2,532 psi) vertical and –10.34 MPa (–1,500 psi) horizontal. After cycling to equilibrium, the boundaries were fixed, and the platens were slowly loaded with uniform vertical stress until the cell stress was 10% greater than the far-field vertical stress, or –19.20 MPa (–2,785 psi). After reaching equilibrium again, the applied loading surfaces of the platens were fixed in the vertical direction. The last phase of the experiment simulated mining-induced loading—that is, the side boundaries remained fixed with zero x-direction velocities, but the top and bottom boundaries were freed from the zero velocity constraint and were loaded slowly until the applied vertical stress was –68.95 MPa (–10,000 psi), and equilibrium was then achieved. An average horizontal stress was calculated and recorded as a history from the model zones (or elements) adjacent to the side boundaries using a volume-weighted method to compensate for varying zone size. The average vertical stress was recorded as a history from the zones adjacent to the top and bottom boundaries using a volume-weighted method. The average cell pressure was calculated from the stresses in the zones adjacent to the applied loading surfaces. After model calculations were completed, the applied stresses where nodes were fixed were verified by extracting and summing the reaction forces and dividing by the area over which they were applied.

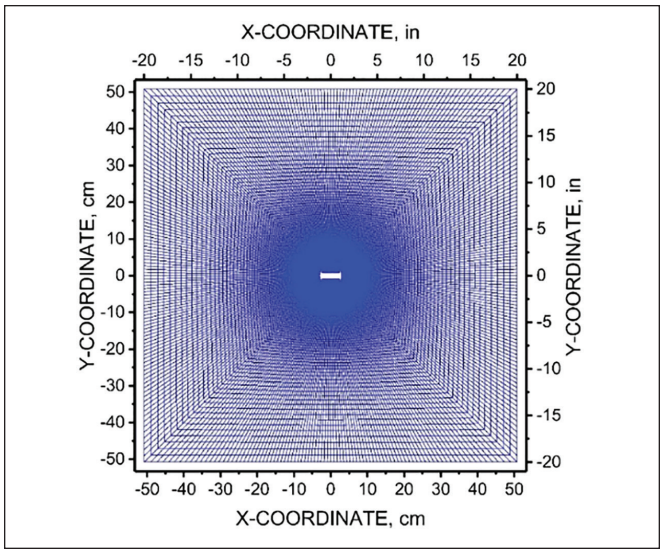

Figure 1. Model grid used to simulate field loading of BPC.

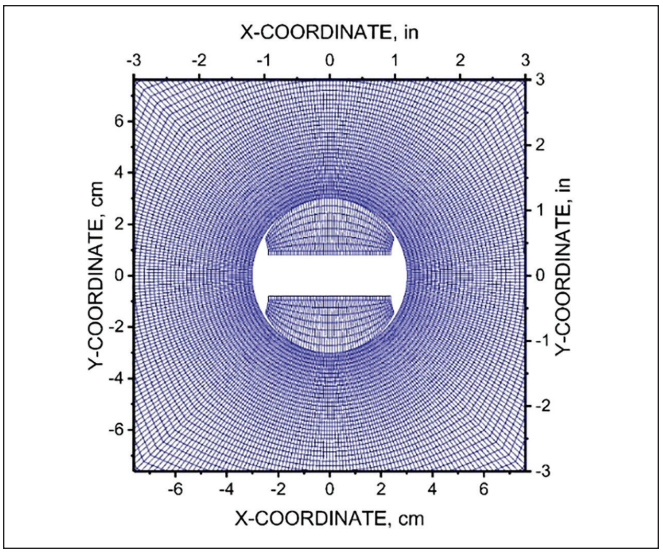

Figure 2. Zoomed-in model grid showing detail of model used to simulate field loading of BPC.

Modeling the BPC in this way causes some differences from reality. For example, system stiffness is not simulated in this way. In reality, the hydraulic system has a comparatively softer stiffness than does the rest of the system and cannot be simulated adequately. Moreover, loading by the flatjack is not uniform. Our attempt to account for part of the hydraulic stiffness was accomplished by setting the stiffness of the zones adjacent to the applied platen loads at half the stiffness of the grout. Although some variation of the stiffness of these rows of zones was tried (22% lower) in an attempt to bring the simulation of the Babcock tests closer to the measured results, this change had insufficient effect to bring the simulated sensitivities with various host materials into line with the measured results. However, the varying area of contact from seating for each laboratory test appear to have a more significant effect than hydraulic stiffness. In reality, to account for the hydraulic stiffness of a specific system installed in the field, we would have to obtain such data from laboratory tests, and then any calibration would be good for that system only. For purposes of this paper, this loading approach for the platens was deemed adequate. Because of these imperfections, among other things, the results of this study should not be used to establish calibration factors for real measurement cases.

To realistically simulate the strength of the coal, variable strength properties were assigned to the coal zones. A skewed normal distribution of UCS was approximated with a triangular distribution of UCS to prevent unrealistically high or low values from being generated, with the peak of the distribution at 12.41 MPa (1,800 psi), the lower limit at 10.34 MPa (1,500 psi), and the upper limit at 24.13 MPa (3,500 psi). This range may represent a stronger coal for a field scale. One might argue whether the scale of our numerical experiment is closer to laboratory scale than to field scale. In that case, we have a weak intact coal. The range may reflect properties of some coals in the western U.S. Regardless, our purpose is not calibration, but to demonstrate the effect of host material inelasticity on the instruments. For this distribution of UCS, the internal friction angle was kept constant at 40°, and the cohesion varied according to the distribution.

Table 1. List of cases modeled.

Case Indicator	Case Descriptor	Critical Plastic Shear Strain	Residual Cohesion as Fraction of Initial Cohesion	Normalized Post-Peak Slope§
Case B	Elastic	NU*	NU	NU
Case C	Elastic-perfectly plastic	NU	NU	NU
Case D	Ductile	0.015	0.85	10
Case E	Moderately ductile	0.010	0.50	50
Case F	Moderately brittle	0.010	0.20	80
Case G	Brittle	0.005	0.10	180

*NU = Not used
§Normalized to the initial cohesion

Six cases were constructed. For Case B, all materials were elastic. Case C was a Mohr-Coulomb model with the post-peak strength behavior being elastic-perfectly plastic. Cases D through G were strain softening cases for the coal and elastic-perfectly plastic for the grout platens. Case Gdil is the same as Case G, but the dilation angle was 10° instead of 0° as it was for all other cases. The descriptions of the cases are listed in Table 1.

To judge whether the model results are sufficiently accurate and representative of an instrument in the hole of an infinite body and to perceive whether these six cases represent enough variation in the stress profile, stress profiles were plotted along three profile lines—along the positive x axis, along the positive y axis, and at a 45° angle between these axes in the positive quadrant. The stress profiles were taken at two stages: (1) at initial stress equilibrium with the borehole but no BPC present, and (2) after the BPC was set and additional loading was applied, simulating additional

loading from mining, and equilibrium was reached. The stress profiles of the Kirsch solution were used to compare to the elastic results. In addition, the objective was to characterize the stress profiles resulting from increasing degrees of post-peak-strength deformation, anticipating some differences among the cases.

Although not shown graphically in this paper, the congruence with the Kirsch solution by the elastic model stresses at initial equilibrium and the spread of stress profiles among the other cases resulting from inelastic behavior give us confidence that the stress profiles are different enough to show whether inelastic behavior affects the response of the BPC. Now, we are prepared to examine how the simulated BPC cell pressure responds to increased vertical stress from the point of the instrument set at a cell pressure of –19.20 MPa (–2,785 psi), which is 10% over the initial vertical stress, a common setting pressure level, according to our knowledge and discussions over many years with other users of the BPC.

Figure 3 shows the state of cohesion at the time of borehole equilibrium before the BPC is inserted and at the time that the BPC is set and the additional load is applied and a new equilibrium is established. Some readers may like to think of state of cohesion in terms of state of fracturing, where a lower cohesion from shear strain represents increased microfracturing. The plots in Figure 3 show three of the cases having a host material constitutive model of strain softening. The range of progression of cohesion deterioration

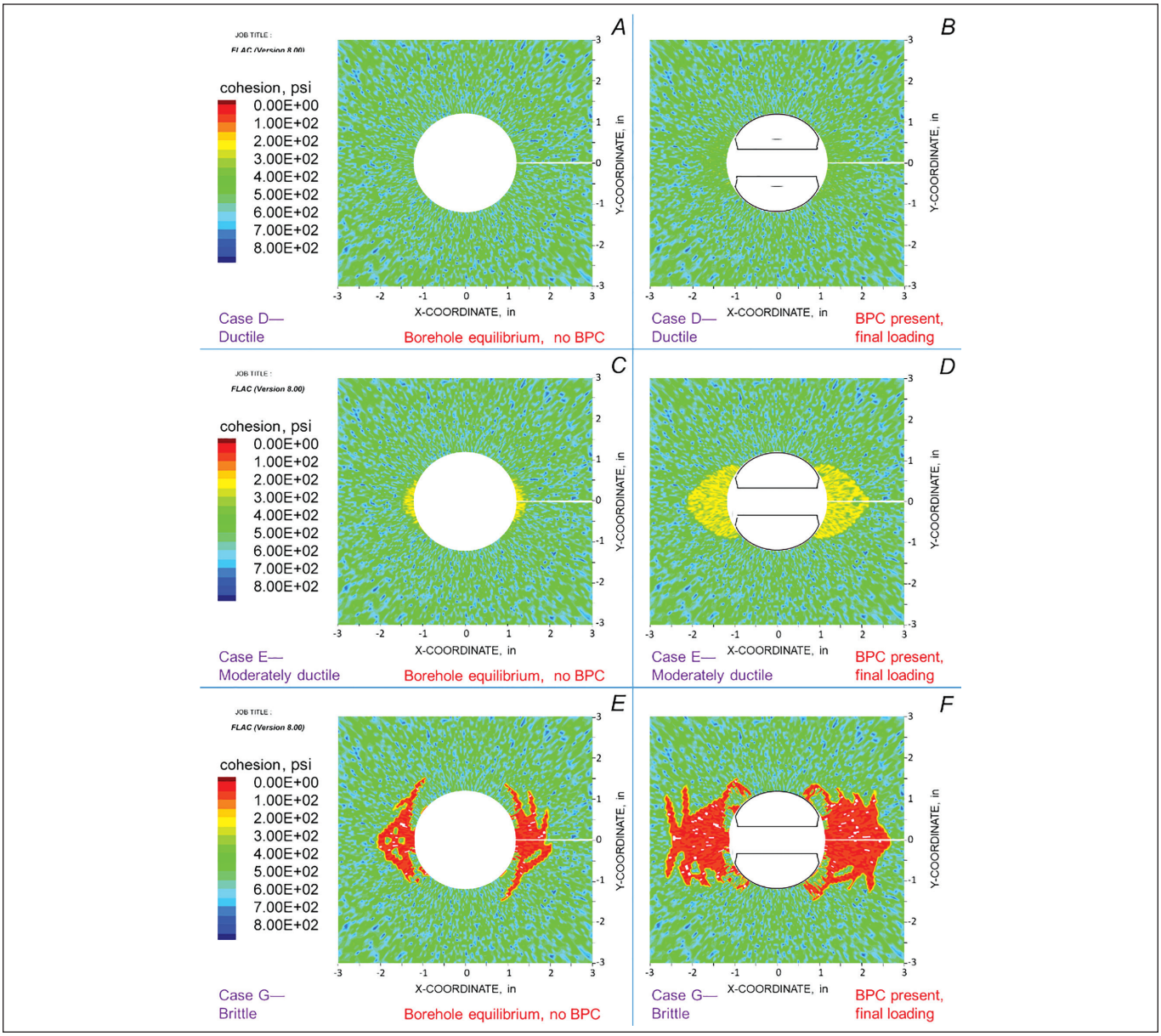

Figure 3. State of cohesion near the borehole for some example BPC models in which the coal has the following strength criteria. *A*, Case D at borehole equilibrium and no BPC; *B*, Case D with BPC set and final loading equilbrium; *C*, Case E at borehole equilibrium and no BPC; *D*, Case E with BPC set and final loading equilbrium; *E*, Case G at borehole equilibrium and no BPC; and *F*, Case G with BPC set and final loading equilbrium.

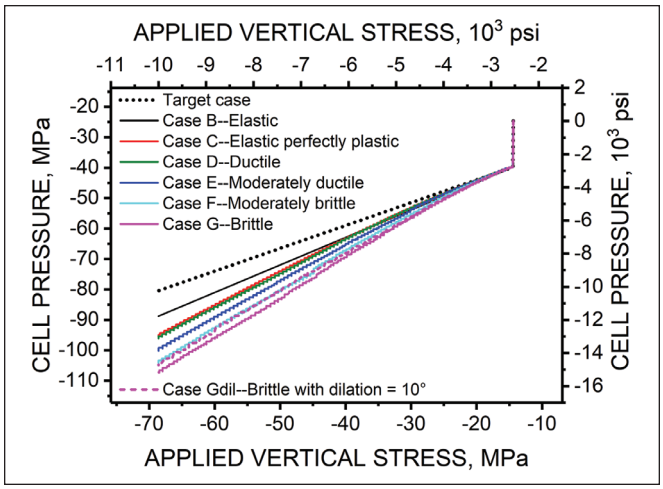

Figure 4. Cell pressure versus applied vertical stress for numerical experiment on the BPC with increasing rate of decrease of post-peak strength stress with plastic shear strain.

is substantial from Case C (not shown, but no significant deterioration) to Case G. Additionally, several cases establish borehole equilibrium when the host material cohesion near the borehole wall has already deteriorated significantly.

Figure 4 shows a plot of cell pressure versus applied vertical stress during the loading cycles from loading the cell to 110% of vertical stress and the subsequent increase of applied vertical stress to –68.95 MPa (–10,000 psi) in compression. In the figure, the "target case" represents a one-to-one correspondence in the response as if the cell pressure change is the same as the applied vertical stress change—an assumption used in several field studies over the years, as mentioned earlier.

Figure 4 clearly shows a progression in the relationship between cell pressure change and applied stress change according to the post-peak strength slope or the degree of plasticity. The elastic-perfectly plastic case (Case C) and the ductile case (Case D) do not show much difference, probably because the amount of plastic shear strain was very small, as verified by Figure 3A–B for the ductile case, where the drop in cohesion was only slight for Case D (ductile). Otherwise, the increased amount of plastic deformation steepens the curve in Figure 4.

The effect of nonlinear, plastic behavior is further shown by a comparison of ratio of the cell pressure increase to the applied vertical stress increase (Table 2). As the amount of plastic deformation increases, this ratio increases significantly. This result suggests that the reason for the cell pressure being higher than possible in the NIOSH study mentioned earlier (NIOSH, 2019a, 2019b) is that the high cell pressure was caused by significant yielding and deterioration of the coal near the borehole wall. Coal, being a very brittle material, likely would react similarly to Case G or Gdil under such initial stress and stress change. However, because the FLAC model used in this experiment was not calibrated to include the contribution of the hydraulic system to stiffness, the ratio amounts in Table 2 may be inflated slightly.

Table 2. Ratio of change of cell pressure to change in vertical stress.

Case	Cell Pressure to Applied Stress Ratio
Case B (elastic)	1.21
Case C (elastic-perfectly plastic)	1.36
Case D (ductile)	1.38
Case E (moderately ductile)	1.48
Case F (moderately brittle)	1.58
Case G (brittle)	1.66
Case Gdil (brittle, dilation = 10°)	1.62

The result for the elastic-perfectly plastic case is within the range found by Su and Hasenfus (1990) in their elastic-perfectly plastic model. In general, the results in the table indicate that estimating stress change with the pre-encapsulated BPC is difficult when loading goes beyond the elastic limit. Users need to be aware of this type of behavior. Estimation of stress change based on this study is not recommended because the models were not calibrated to a real system response. However, stress change profiles extracted through established means still provide qualitative information. If accurate stress change profiles are desired when the host medium is likely to have an inelastic response, the user could consider other options.

Biaxial Stressmeter Simulation of Hypothetical Field Loading

The biaxial stressmeter data reduction scheme is based on an elastic solution by Savin (1961) for a ring welded fully to the hole surface in a plate. We will not detail the solution or the data reduction scheme here. The latter is detailed well in the instrument manual (Geokon, 2019).

The BSM numerical model was constructed much like that for the BPC, and the loading experiment was very similar. The boundaries of the rock and borehole in the model were the same as in the model of the BPC. Figure 5 is a zoomed-in view of the model grid showing constitutive models for the coal, grout, and the hollow cylinder of the instrument. However, for the BPC, there was a frictional interface between the platens and the coal. For this experiment, perfect bonding was assumed between the grout and the coal and between the grout and the instrument. Loading was similar. The initial stress state before insertion of grout and instrument was –19.20 MPa (–2,785 psi) of applied vertical stress and –10.34 MPa (–1,500 psi) of applied horizontal stress. Mine Backer Grout that was used for the BPC platens was assumed to be the grout in this model. In reality, Mine Backer Grout does not have the setting time needed for installation. However, for this experiment we choose to use it because we had measured properties, it makes the experiment similar to that of the BPC, and appropriate grouts such as Special Grout 400 is likely to have similar properties, even if the modulus might be stiffer. The result of this numerical experiment, then, would provide a conservative result, meaning that actual performance of the instrument should be better than the numerical result. After reaching equilibrium around the borehole, the instrument and grout were installed, the side boundaries were fixed with zero velocity in the x-direction, and the upper and lower boundary stresses were increased slowly to

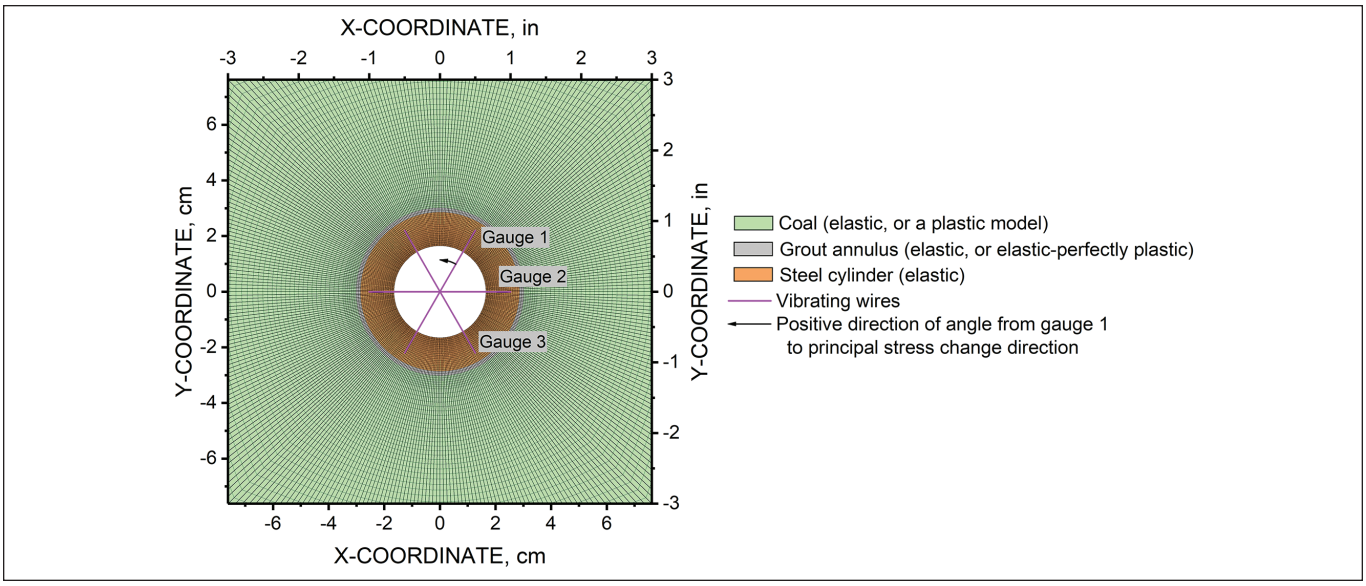

Figure 5. Zoomed-in view of the FLAC model grid of the biaxial stressmeter, with materials and constitutive models indicated.

the final state of –68.95 MPa (–10,000 psi), followed by cycling to equilibrium.

The same cases of coal behavior that were simulated for the BPC, listed in Table 1, were simulated also for the biaxial stressmeter. Before we examine the stress change as calculated from simulated measurements of the BSM, it is useful to examine the stress profiles as we did for the BPC. Stress profiles were taken from the models and normal stresses along the positive axes. Although not shown in this paper, the cases of the borehole without the BSM installed, the elastic case stress profiles show very little deviation from the Kirsch solution. Increasing plasticity modifies the stress profiles, particularly in the vicinity of the borehole. The inclusion of the BSM and increasing the vertical stress, on the right-hand side of the figures, shows significant deviations in some of the stress profiles in the host medium. There is enough scatter in the stress profiles to indicate the presence of various degrees of post-peak strength behavior. The trend is that the stress near the borehole wall is reduced so that the location of the peak stress is forced to be further from the borehole wall.

Comparing these stress profiles with the corresponding profiles of the BPC, the scatter of the stress profiles with increasing plastic behavior is similar. However, the ends of the vibrating wires in the BSM are located at a radius of 2.54cm (1.00in). Consequently, there is not much difference in the stress profiles between the cases at that radius for the BSM. Moreover, the deterioration in cohesion between the initial hole state and the final loading state with the BSM installed is minimal in each case, as shown by the example cases in Figure 6. The reason for the minimal deterioration in cohesion appears to be the significant confinement that the stiff, hollow cylinder provides the host material. By comparison, the BPC only provides confinement in the vertical direction, whereas the BSM provides confinement all the way around the borehole. The confining effect is very evident if the changes in Figure 6 are compared to the cohesion deterioration shown in Figure 3.

Finally, there are some minor differences in stress profile and deterioration of cohesion between Case G and Case Gdil—the brittle cases with dilation at 0° and 10°, respectively. The differences in deterioration of cohesion are not shown here, but the drop in cohesion of Case Gdil was slightly more intense. Thus, the results of this study, performed mostly with a dilation angle of 0° do not seem to be narrowly defined for the condition of 0°. Even so, we cannot rule out that a dilatant material could cause increased deviation from the elastic solution. But the differences between the Case G and Case Gdil profiles seem minimal, even if they are not insignificant. For clarity, in this study we used the prevailing sign convention of mechanics instead of that of mining geomechanics—that tensile stress change is positive and compressive change is negative.

The results of stress change determination from model displacements—that is, from diameter changes at an initial radius of 2.54cm (1in) at 60°, 0°, and –60° from the x-axis—were used to calculate stress change. The results of determining the secondary principal stresses, P and Q and their directions, are listed in Table 3, while the errors relative to the target condition are noted in Table 4. The results are very good for determining the principal stress change in the direction of the applied "mining stress"—that is, Q. For P, the results range from 2.60% to 6.70% more negative (compressive) than the target amount for that component—which includes the Poisson effect of the additional mining stress of –49.75 MPa (–7,215 psi), or –16.58 MPa (–2,405 psi).

DISCUSSION

The results calculating stress change from the simulated BSM under various conditions of the host medium appears to produce very accurate results with the elastic data reduction equations. The degree of plasticity seems to have minimal effect because of the confinement exerted by the instrument itself in all directions.

The cause of relatively high error in the secondary principal stress, P, as determined with the BSM in the models needs some investigation.

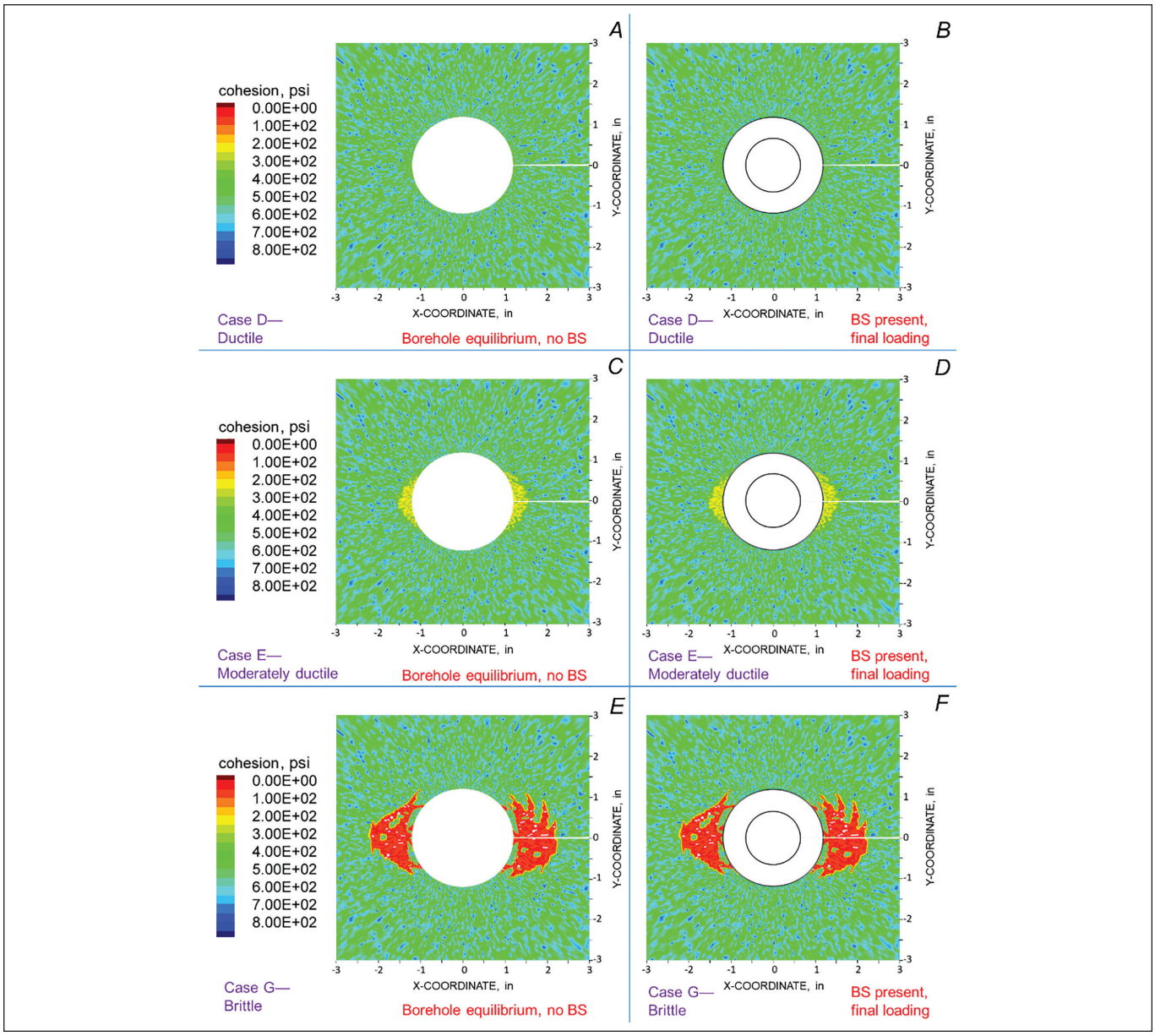

Figure 6. State of cohesion near the borehole for some example biaxial stressmeter models in which the coal has the following strength criteria. *A*, Case D at borehole equilibrium and no instrument; *B*, Case D with instrument installed and final loading equilbrium; *C*, Case E at borehole equilibrium and no instrument; *D*, Case E with instrument installed and final loading equilbrium; *E*, Case G at borehole equilibrium and no instrument; and *F*, Case G with instrument installed and final loading equilbrium.

Table 3. Major, P, and minor, Q, secondary principal stress changes calculated with simulated biaxial stressmeter in FLAC model.

Model	P, MPa	P, psi	P Direction, °	Q, MPa	Q, psi	Q Direction, °
Target	–16.5819	–2405.00	–60.00	–49.7457	–7215.00	30.00
Case B—Elastic	–17.6708	–2562.93	–60.00	–49.5796	–7190.92	30.00
Case C—Elastic-perfectly plastic	–17.6283	–2556.78	–60.00	–49.5831	–7191.42	30.00
Case D—Ductile	–17.6230	–2556.01	–60.00	–49.5837	–7191.42	30.00
Case E—Moderately ductile	–17.6936	–2566.23	–60.01	–49.7060	–7209.24	29.99
Case F—Moderately brittle	–17.2774	–2505.88	–59.99	–49.4947	–7178.60	30.01
Case G—Brittle	–17.3897	–2522.17	–59.99	–50.0940	–7265.52	30.02
Case Gdil—Brittle with dilation = 10°	–17.0125	–2467.46	–60.01	–49.9560	–7245.51	29.99

Table 4. Errors of calculated determinations of stress change from biaxial stressmeter deformation in FLAC models.

Model	Error in P. %	Error in P Direction, %	Error in Q, %	Error in Q Direction, %
Case B—Elastic	6.57	0.00	–0.33	0.00
Case C—Elastic-perfectly plastic	6.31	0.00	–0.33	0.00
Case D—Ductile	6.28	0.00	–0.33	0.00
Case E—Moderately ductile	6.70	0.02	–0.08	–0.04
Case F—Moderately brittle	4.19	–0.02	–0.50	0.04
Case G—Brittle	4.87	–0.03	0.70	0.06
Case Gdil—Brittle with dilation = 10°	2.60	0.02	0.42	–0.04

Table 5. Results of model having coal substituted for the grout annulus.

Model	P, MPa	P, psi	P Direction, °	Q, MPa	Q, psi	Q Direction, °
Target	–16.5819	–2405.00	–60.00	–49.7457	–7215.00	30.00
Case B—Elastic with no grout annulus	–16.6187	–2510.34	–60.00	–49.8360	–7228.11	30.00
Error	0.2221%	0.2221%	–0.0002%	0.1817%	0.1817%	0.0004%

The source of error was the difference in conditions between an actual installation and the geometry of the case solved by Savin—an elastic ring perfectly welded to the hole in an elastic plate. In reality, we have an annulus of grout, so that there are three materials instead of two. We reran the Case B model (elastic case), but with the annulus of grout converted to coal material. The results, listed in Table 5, show that simulating the problem of the Savin solution more exactly results in very little error in the model results compared to the target stress changes and directions. Therefore, it appears that a grout annulus with different stiffness compared to the host material can cause some error in determining the secondary major principal stress change, P.

The pre-encapsulated BPC provides no similar degree of confinement, especially in the direction where the greatest amount of plastic deformation occurs—at the side of the borehole. As a result, further loading causes further plastic shear deformation, particularly at the sides of the borehole where stress concentration from additional applied stress is concentrated.

The main difference between the instruments is how they respond to increasingly plastic behavior. The encapsulated BPC is significantly affected by the post-peak behavior of the host material. On the other hand, the BSM elastic analysis seems to produce similar results, no matter the case of post-peak behavior in the range that we tested. The difference is evident in Figure 6, where the deterioration in cohesion of the host material was minimal because of the significant confinement of the hollow cylinder.

The question then becomes what is the effect on the BPC that is not pre-encapsulated, but is grouted in place. Without doing the experiments, our assessment is that it is somewhere between the pre-encapsulated BPC results and the BSM results. Certainly, there is slightly more confinement compared to the pre-encapsulated BPC. However, the flatjack is still applying pressure in one direction, such that the lateral confinement may still be insignificant. Only further testing can determine that response.

The results of this numerical experiment suggest that obtaining an accurate stress change profile measured by the BPC is difficult if there is any plastic shear deformation. On the other hand, the biaxial stressmeter provides significant confinement, which largely prevents additional significant plastic shear deformation with additional stress resulting from mining.

CONCLUSION

The attempt to reproduce the laboratory results of Babcock (1986) with a numerical model using FLAC was not as successful as hoped because the numerical model did not account for actual loading conditions—that is, the model used a uniform stress on the grout platens instead of trying to account for the effect of loading with a flatjack and the same BPC was used in all tests, in increasing order of setting pressure. The BPC had to be compressed to insert the cell in the hole of a new material. Therefore, some seating of the flatjack took place in each laboratory test. The change in area associated with this seating and the change in area by applying outside stress above the setting pressure were unknown. Although no attempt was made to try to simulate this effect more closely with FLAC, the uniform load and fixing of the inner surface of the platens provides a reasonable basis from which to investigate the effect of yielded host medium on the cell. The greater agreement of the delta pressure ratio reported in Table 1 supports this point. As such, the results of this study should not be used for a general calibration of the BPC.

The numerical experiments that were conducted showed a wide range in the effect of post-peak strength behavior on the measurement of the stress field. Such behavior was even initially apparent near the borehole before any instrument was installed. Thus, the experiments were well suited for determining the effect of various post-peak strength behavior on the response of the BPC and the BSM.

The model results show that the BPC response is significantly affected by plastic behavior, such that the data reduction schemes

based on elastic response are no longer applicable. The platens provide no lateral confinement, allowing plastic deformation to take place with additional stress resulting from mining. Because of the difficulty in assessing the shape of the post-peak stress-strain curve, accurately profiling stress change as mining progresses is difficult when the yield point of the plastic material is surpassed. From our numerical experiments, the ratio of cell pressure change to applied stress change may range from 1.21 to 1.66 or more depending on the brittleness of the material and the critical strain. We do not conclude that making BPC measurements is not valuable. For example, the relative response between BPCs across a pillar is very indicative of pillar behavior, and its value in determining load transfer distance has already been well demonstrated (Larson and Whyatt, 2012; NIOSH, 2019a, 2019b).

On the other hand, model results indicate that the BSM provides significant confinement over the entire circumference of the borehole to the degree that additional plastic deformation calculated by the models is minimal with increased stress resulting from mining. As a result, the elastic solution still provides a reasonably accurate measurement of the secondary principal stress system. The overestimate of P from the model results is likely the result of nonuniform reaction forces at fixed side boundaries and possibly the first-order zones used in the finite difference scheme of FLAC. The implications of these results is that when conducting field studies, the BSM is the better instrument for accurately monitoring stress change when the host material near the borehole is loaded beyond its elastic range. This implication needs to be verified by laboratory testing of physical installations.

For the future, the BPC model that is not pre-encapsulated needs investigation to determine the effect of plastic deformation on its results. Finally, the ability of CSIRO's hollow inclusion stress cell as a stress monitor needs further investigation, including separation of the effects of temperature and creep from response resulting from applied stress change.

DISCLAIMER

The findings and conclusions in this report are those of the author(s) and do not necessarily represent the official position of the National Institute for Occupational Safety and Health, Centers for Disease Control and Prevention. Mention of any company or product does not constitute endorsement by NIOSH.

ACKNOWLEDGMENTS

The authors would like to thank Brad Seymour and Daniel Su of NIOSH, and Barrie Sellers of Geokon for helpful discussions and comments concerning this manuscript.

REFERENCES

Babcock, C.O. (1986). "Equations for the analysis of borehole pressure cell data." In: Hartman, H.L. Ed. *Rock Mechanics: Key to Energy Production, Proceedings of the 27th U.S. Symposium on Rock Mechanics*. (Tuscaloosa, AL: June 23–25, 1986). Littleton, CO: Society of Mining Engineers.

DeMarco, M.J., Koehler, J.R., and Lu, P.H. (1988). Characterization of chain pillar stability in a deep western coal mine — a case study. *Mining Eng. 40*(12): 1115–1119.

Earth Sciences (2019). 3D Stress CSIRO Analogue HI Cell. Earth Sciences. http://www.essearth.com/product/3d-stress-cell-csiro-hollow-inclusion-hi-cell/.

Estey, L.H. (1995). "Overview of USBM mcroseismic instrumentation and research for rock-burst mitigation at the Galena Mine, 1987–1993." In: Maleki, H., et al. Eds. *Proceedings: Mechanics and Mitigation of Violent Failure in Coal and Hard-Rock Mines*. (Special Publication 01-95). U.S. Department of the Interior, Bureau of Mines (USBM).

Geokon (2018a). Borehole pressure cells. Geokon, Inc. http://www.geokon.com/3200.

Geokon (2018b). Biaxial stressmeters. Geokon, Inc. http://www.geokon.com/4350.

Geokon (2019). *Instruction manual: Model 4350BX biaxial stressmeter*. Lebanon, NH: Geokon, Inc.

Itasca Consulting Group (2016). FLAC—Fast Lagrangian Analysis of Continua, ver. 8.0. Minneapolis, MN: Itasca Consulting Group, Inc.

Koehler, J.R., DeMarco, M.J., Marshall, R.J., and Fielder, J. (1996). "Performance evaluation of a cable bolted yield-abutment gate road system at the Crandall Canyon No. 1 Mine, Genwal Resources, Inc., Huntington, Utah." In: Ozdemir, L., et al. Eds. *Proceedings: 15th International Conference on Ground Control in Mining*. (Golden, CO: August 13–15, 1996). Golden, CO: Colorado School of Mines.

Larson, M.K., Stewart, C.L., Stevenson, M., King, M.E., and Signer, S.P. (1995). "A case study of a deformation mechanism around a two-entry gateroad system involving probable time-dependent deformation." In: Peng, S.S. Ed. *Proceedings of 14th International Conference on Ground Control in Mining*. (Morgantown, WV: August 1–3, 1995). Morgantown, WV: West Virginia University.

Larson, M.K., Tesarik, D.R., Seymour, J.B., and Rains, R.L. (2000). "Instruments for monitoring stability of underground openings." In: Mark, C., et al. Eds. *Proceedings: New Technology for Coal Mine Roof Support*. (NIOSH Information Circular 9453: 2000). Pittsburgh, PA: U.S. Department of Health and Human Services.

Larson, M.K., and Whyatt, J.K. (2012). "Load transfer distance calibration of a coal panel scale model: A case study." In: Barczak, T., et al. Eds. *Proceedings of the 31st International Conference on Ground Control in Mining*. (Morgantown, WV: July 31–August 2, 2012). Morgantown, WV: West Virginia University.

Lu, P.H. (1984). "Mining-induced stress measurement with hydraulic borehole pressure cells." In: Dowding, C.H., and Singh, M.M. Eds. *Rock Mechanics in Productivity and Protection, Proceedings: Twenty-Fifth Symposium on Rock Mechanics*. (Evanston, IL: June 25–27, 1984). New York, NY: Society of Mining Engineers.

Lu, P.H. (1986). "Biaxial-loading measurement for mining-pillar stability evaluation — case studies." In: *Proceedings of the International Symposium on Application of Rock Characterization Techniques in Mine Design*. (New Orleans, LA: March 2–6, 1986). Littleton, CO: Society of Mining Engineers, AIME.

NIOSH (2019a). *Ground stress resulting from mining (part 1): Measurements and observations at two western U.S. longwall mines*. By Larson, M.K., Lawson, H.E., Zahl, E.G., and Jones, T.H. Report of Investigations, submitted for publication. Pittsburgh, PA: U.S. Department of Health and Human Services, Centers for Disease Control and Prevention, National Institute for Occupational Safety and Health, DHHS (NIOSH).

NIOSH (2019b). *Ground stress resulting from mining (part 2): Calibrating and verifying longwall stress models*. By Larson, M.K., Tesarik, D.R., and Johnson, J.C. Report of Investigation, submitted for publication. Pittsburgh, PA: U.S. Department of Health and Human Services, Centers for Disease Control and Prevention, National Institute for Occupational Safety and Health, DHHS (NIOSH).

Pariseau, W.G. (2007). *Finite element analysis of inter-panel barrier pillar width at the Aberdeen (Tower) Mine*. Department report, August 30, 2007. Salt Lake City, UT: University of Utah.

Pariseau, W.G., McCarter, M.K., and McKenzie, J. (2008). "Inter-panel barrier pillar study in a deep Utah coal mine." In: *Proceedings: 42nd U.S. Rock Mechanics Symposium, 2nd U.S. Canada Rock Mechanics Symposium.* (San Francisco, CA: June 29–July 2, 2008). Alexandria, VA: American Rock Mechanics Association.

RST Instruments (2018). Borehole pressure cell. https://www .rstinstruments.com/Borehole-Pressure-Cell.html.

Savin, G.N. (1961). *Stress Concentration Around Holes, By G.N. Savin.* . trans. Gros, E., *International series of monographs in aeromautics and astronautics. Division 1: Solid and structural mechanics*. V. 1. Oxford: Pergamon Press, 441 pp.

Sellers, J.B. (1970). The measurement of rock stress changes using hydraulic borehole gages. *Int. J. Rock Mech. Min. Sci.,* 7(4): 423–435.

Su, D., and Hasenfus, G.J. (1990). "Intrinsic response of borehole pressure cells laboratory calibrations and nonlinear FEM simulation." In: Peng, S.S. Ed. *Proceedings: Ninth International Conference on Ground Control in Mining*. (Morgantown, WV: June 4–6, 1990). Morgantown, WV: West Virginia University.

Tadolini, S.C. (2019). Phone conversation between Steve Tadolini and Larson, M. K., April 18.

Tadolini, S.C., and Barczak, T.M. (2008). "Rock mass behavior and support response in a longwall panel pre-driven recovery room." In: Stacey, T.R., and Malan, D.F. Eds. *Proceedings of the 6th International Symposium on Ground Support in Mining and Civil Engineering Construction*. (Cape Town, Republic of South Africa: March 30–April 3, 2008). Johannesburg, Republic of South Africa: The South African Institute of Mining and Metallurgy.

USBM (1964). *Development of a rock stress monitoring station based on the flat slot method of measuring existing rock stress*. By Panek, L.A. and Stock, J.A. Report of Investigations 6537. Pittsburgh, PA: U.S. Department of the Interior, Bureau of Mines (USBM).

USBM (1995). *Longwall gate road stability in a steeply pitching thick coal seam with a weak roof*. By Barron, L.R., and DeMarco, M.J. Report of Investigations 9580. Pittsburgh, PA: U.S. Department of the Interior, Bureau of Mines (USBM).

Vandergrift, T., and Conover, D. (2010). "Assessment of gate road loading under deep western U.S. conditions." In: Mark, C., Barczak, T., and Esterhuizen, G.S. Eds. *Proceedings: 3rd International Conference on Coal Pillar Mechanics and Design*. (Morgantown, WV: July 26, 2010). Morgantown, WV: West Virginia University.

Westman, E.C., Friedel, M.J., Williams, E.M., and Jackson, M.J. (1995). "Seismic tomography to image coal structure stress distribution." In: Maleki, H., et al. Eds. *Proceedings: Mechanics and Mitigation of Violent Failure in Coal and Hard-Rock Mines*. (Special Publication 01-95). U.S. Department of the Interior, Bureau of Mines (USBM).

Westman, E.C., Molka, R.J., and Conrad, W.J. (2016). "Ground control monitoring of retreat room-and-pillar mine in Central Appalachia." In: Barczak, T., et al. Eds. *Procedings: 35th International Conference on Ground Control in Mining*. (Morgantown, WV: July 26–28, 2016). Morgantown, WV: West Virginia University.

Worotnicki, G., and Walton, R.J. (1976). "Triaxial 'hollow inclusion' gauges for determination of rock stresses in situ." In" *Investigation of Stress in Rock. Advances in Stress Measurement: Proceedings of the I.S.R.M. Symposium. National Conference Publication No. 76/4 Supplement*. (Sydney: August 11–13, 1976). Canberra, Australia: The Institution of Engineers,.

Wright, F.D., Howell, R.C., and Dearinger, J.A. (1979). *Rock mechanics study of shortwall mining*. Contract No. U.S. D.O.E. ET-73-C-01-9010 (formerly U.S.B.M. H0133039), April 30, 1979. Lexington, KY.

PROCEEDINGS OF THE 38th International Conference ON GROUND CONTROL IN MINING

ICGCM 2019

Edited by

Ted Klemetti | Brijes Mishra | Heather Lawson | Michael Murphy | Kyle Perry

Published by the
Society for Mining, Metallurgy & Exploration

Society for Mining, Metallurgy & Exploration (SME)
12999 E. Adam Aircraft Circle
Englewood, Colorado, USA 80112
(303) 948-4200 / (800) 763-3132
www.smenet.org

The Society for Mining, Metallurgy & Exploration (SME) is a professional society whose more than 15,000 members represents all professionals serving the minerals industry in more than 100 countries. SME members include engineers, geologists, metallurgists, educators, students and researchers. SME advances the worldwide mining and underground construction community through information exchange and professional development.

ISBN 978-0-87335-472-1